

Molecular Characterization of *Pax6*^{2Neu} Through *Pax6*^{10Neu}: An Extension of the *Pax6* Allelic Series and the Identification of Two Possible Hypomorph Alleles in the Mouse *Mus musculus*

Jack Favor,* Heiko Peters,*¹ Thomas Hermann,[†] Wolfgang Schmahl,[‡] Bimal Chatterjee,*
Angelika Neuhäuser-Klaus* and Rodica Sandulache*

*Institute of Mammalian Genetics, GSF-Research Center for Environment and Health, Neuherberg D-85764, Germany,
[†]Memorial Sloan-Kettering Cancer Center, New York, New York 10021 and [‡]Lehrstuhl für Allgemeine Pathologie und
Neuropathologie, Tierärztliche Fakultät, Ludwig-Maximilians-Universität, München D-80539, Germany

Manuscript received April 27, 2001
Accepted for publication September 28, 2001

ABSTRACT

Phenotype-based mutagenesis experiments will increase the mouse mutant resource, generating mutations at previously unmarked loci as well as extending the allelic series at known loci. Mapping, molecular characterization, and phenotypic analysis of nine independent *Pax6* mutations of the mouse recovered in mutagenesis experiments is presented. Seven mutations result in premature termination of translation and all express phenotypes characteristic of null alleles, suggesting that *Pax6* function requires all domains to be intact. Of major interest is the identification of two possible hypomorph mutations: Heterozygotes express less severe phenotypes and homozygotes develop rudimentary eyes and nasal processes and survive up to 36 hr after birth. *Pax6*^{4Neu} results in an amino acid substitution within the third helix of the homeodomain. Three-dimensional modeling indicates that the amino acid substitution interrupts the homeodomain recognition α -helix, which is critical for DNA binding. Whereas cooperative dimer binding of the mutant homeodomain to a paired-class DNA target sequence was eliminated, weak monomer binding was observed. Thus, a residual function of the mutated homeodomain may explain the hypomorphic nature of the *Pax6*^{4Neu} allele. *Pax6*^{7Neu} is a base pair substitution in the Kozak sequence and results in a reduced level of *Pax6* translation product. The *Pax6*^{4Neu} and *Pax6*^{7Neu} alleles may be very useful for gene-dosage studies.

IN the mouse a number of large-scale mutagenesis screens have been undertaken to systematically recover mutations with relevant phenotypes to complement the forthcoming genome sequence data and to provide the genetic variants to initiate functional genetic studies (HRABÉ DE ANGELIS *et al.* 2000; NOLAN *et al.* 2000). We have conducted an extensive series of mutagenesis experiments to recover dominant mutations that affect eye morphology (FAVOR and NEUHÄUSER-KLAUS 2000). A total of 192 independent mutations are available for genetic and molecular analyses, which represents one of the largest collections of mutations affecting the development and function of a defined organ. We are systematically mapping all recovered mutations to identify the genes/loci responsible for eye development. Our results to date indicate that the most mutable locus is at chromosome 2, centimorgan 58 in the vicinity of the *Pax6* gene, which is known to function in eye development. This combination of chromosomal location and the known involve-

ment of *Pax6* in eye development suggested that *Pax6* is the candidate gene affected in this large group of mutations.

The mouse *Pax6* gene belongs to the family of paired-box-containing genes, which function as transcription factors regulating developmental processes. *Pax6* encodes a protein with both a paired domain and homeodomain, separated by a linker segment, and followed by a C-terminal proline-, serine-, and threonine-rich region (WALTHER and GRUSS 1991). The highly conserved paired domain and homeodomain are DNA-binding domains while the proline-, serine-, and threonine-rich domain functions in transcriptional activation (GLASER *et al.* 1994). Mutant analyses have shown that *Pax6* plays a role in the development of the eye (THEILER *et al.* 1978; HOGAN *et al.* 1988), nasal derivatives (HOGAN *et al.* 1988; HEINZMANN *et al.* 1991; GRINDLEY *et al.* 1995; QUINN *et al.* 1996), additional craniofacial traits (KAUFMAN *et al.* 1995), the central nervous system (CNS; SCHMAHL *et al.* 1993; GRINDLEY *et al.* 1997; STOYKOVA *et al.* 1996, 1997, 2000; GÖTZ *et al.* 1998), the pancreas (ST-ONGE *et al.* 1997), and the pituitary gland (BENTLEY *et al.* 1999; KIOUSSI *et al.* 1999). Heterozygous carriers of *Pax6* null mutations express phenotypic effects, which suggests that a defined concentration of *Pax6* protein activity is necessary for normal development (HILL *et*

Corresponding author: Jack Favor, Institute of Mammalian Genetics, GSF-Research Center for Environment and Health, Ingolstädter Landstr. 1, D-85764, Neuherberg, Germany. E-mail: favor@gsf.de

¹ Present address: University of Newcastle upon Tyne, Institute of Human Genetics, Newcastle upon Tyne, NE1 7RU United Kingdom.

al. 1991). This suggestion is supported by studies in which the wild-type *Pax6* allele was overexpressed and resulted in abnormal eye development (SCHEDL *et al.* 1996).

Human patients heterozygous for *PAX6* mutant alleles express eye abnormalities similar to those observed in the mouse (BROWN *et al.* 1998; PROSSER and VAN HEYNINGEN 1998). Most described *PAX6* mutant alleles result in premature termination of translation. The underrepresentation of missense mutations may be due to the fact that hypomorph alleles likely result in a less severe phenotype and patients who carry hypomorph alleles might not have been included in a mutation screen.

The identification of *Pax6* hypomorph alleles in a laboratory animal would be useful to experimentally address the question of Pax6 protein activity dosage and phenotypic defects. Here we report nine new *Pax6* mutant alleles in the mouse. Seven mutations result in a truncated gene product. Of major interest is the identification of two possible hypomorph alleles. One is an amino acid substitution in the homeodomain. The second is a base pair substitution in the Kozak sequence.

MATERIALS AND METHODS

Animals: All inbred strain (C3H, C57BL/6, 102), F₁ hybrid (102×C3H) and Tester-stock animals were obtained from breeding colonies maintained by the GSF-Department of Animal Resources at Neuherberg.

Mutation recovery: Mutants were recovered in the offspring of (102×C3H)F₁ hybrid or C3H males that were mutagenically treated and mated to untreated Tester-stock or C3H females, respectively. Prior to the initiation of the mutagenesis experiments, all parental animals were ophthalmologically examined and only those that did not express an eye morphological abnormality were employed in order to eliminate any preexisting eye mutations.

Ophthalmological examination: Mice were examined biomicroscopically for eye abnormalities at weaning. Pupils were dilated with a 1% atropin solution applied to the eyes at least 10 min prior to examination. Both eyes of the mice were examined by slit lamp biomicroscopy (Zeiss SLM30) at ×48 magnification with a narrow beam slit lamp illumination at a 25°–30° angle from the direction of observation.

Genetic confirmation crosses: The recovered presumed dominant eye mutants were outcrossed to wild-type strain 102, C3H, or (102×C3H)F₁ partners and at least 20 offspring were ophthalmologically examined for transmission of the specific eye abnormality. The offspring were carefully examined to arrive at a more complete description of the phenotype expressed by heterozygous carriers. A detailed consideration of the ophthalmological examination procedures and genetic confirmation test has been published (FAVOR 1983). All confirmed mutations were maintained by outcrossing heterozygous carriers to homozygous wild-type partners. Before initiating the mapping experiments each mutation was backcrossed at least 10 generations to strain C3H.

Mapping and allelism tests: Complete details of our mapping procedures have been published recently (FAVOR *et al.* 1997). Segregation data were analyzed with Map Manager, Version 2.6.5 (MANLY 1993), and the gene order was determined by minimizing the number of multiple crossovers. Allelism was tested by mating heterozygous carriers of an un-

mapped mutation (ENU-65 or ENU-5011) to heterozygous *Pax6*^{Sey-Neu}/+ mice. Pregnant females were dissected at stages E15 to E17 and embryos were classified for the typical homozygote mutant *Pax6* phenotype indicative of noncomplementation (anophthalmia and craniofacial abnormalities).

RT-PCR and sequence analysis: Total RNA was isolated from heads of E15 embryos expressing the typical wild-type or homozygous mutant *Pax6* phenotype recovered in *inter se* crosses of heterozygotes using the RNeasy kit (QIAGEN, Chatsworth, CA). RNA was reverse transcribed and the entire coding region was PCR amplified with a Titan one Tube RT-PCR system (Roche Diagnostics, Mannheim, Germany) as recommended by the supplier. Two overlapping primer sets, A, 5'-CAGAA GACTTTAACCAAGGGC [nucleotide (nt) 33–53] and 5'-AT CCTTAGTTTATCATACATGCCG (nt 647–623), and B, 5'-AACAGAGTTCTTCGCAACCTGG (nt 573–595) and 5'-GCT GTGTCACATAGTCATTGGC (nt 1545–1522), were used for the amplification of the *Pax6* cDNA. The PCR products were HPLC purified and sequenced with a Taq Dye-Deoxy terminator cycle sequencing kit by SequiServe (Vaterstetten, Germany). Additional primers were used for the complete sequencing of the coding region as well as for the confirmation of the mutation employing genomic DNA as a template.

Numbering of the *Pax6* nucleotides and codons/amino acids follows that of WALTHER and GRUSS (1991).

Assay for nasal development: To assay the extent of nasal development in *Pax6* mutant mice we utilized the *Pax9*^{lacZ} reporter gene, which is expressed in nasal mesenchyme (PETERS *et al.* 1998). Double heterozygotes, consisting of *Pax9*^{lacZ}/+ with *Pax6*^{Sey-Neu}/+ or *Pax6*^{4Neu}/+, were constructed and bred to heterozygous carriers of the respective *Pax6* mutant allele. Embryos (E12) were identified as homozygous wild type and heterozygous or homozygous mutant at the *Pax6* locus by phenotype. Heterozygous *Pax9*^{lacZ} carriers were identified by a PCR assay as previously described (PETERS *et al.* 1998). Whole mount *Pax9*^{lacZ}/+ embryos were stained with X-Gal for 8–12 hr according to established protocols (GOSSLER and ZACHGO 1993). To completely visualize *Pax9*^{lacZ} expression, embryos were dehydrated in methanol and cleared with benzyl benzoate/benzyl alcohol.

Assay for eye phenotype: Offspring from the cross-mutant heterozygote with inbred strain C3H/J were ophthalmologically examined at 21 days of age and categorized for the degree of lens/corneal opacity. At 30 days of age the offspring were sacrificed by cervical dislocation, and eyes were enucleated, washed once in PBS, rinsed in H₂O, blotted dry on filter paper, and weighed. Eye weight data were statistically analyzed by Factorial ANOVA, General Linear Models Procedure, employing SAS Software release 6.12 (Cary, NC).

Histology: Pregnant females from *Pax6*^{4Neu}/+ or *Pax6*^{7Neu}/+ *inter se* crosses were sacrificed on day 16 postconception and embryos assigned a genotype on the basis of phenotype (heterozygotes have a slightly smaller eye with distorted shape of the pupil; homozygous mutants are anophthalmic). Embryos were fixed in 10% buffered formalin, and heads were embedded in paraffin and serially sectioned (coronal) at 5 μm. Sections were stained with hematoxylin and eosin.

Three-dimensional modeling: A three-dimensional model of the *Pax6* homeodomain (Leu1 through Glu60) was constructed by homology modeling using the atomic coordinates of the homeodomains of the genes *paired* (WILSON *et al.* 1995), *Antennapedia* (QIAN *et al.* 1994b), *VND/NK-2* (TSAO *et al.* 1995), *engrailed* (KISSINGER *et al.* 1990), and *Fushi Tarazu* (QIAN *et al.* 1994a). Protein sequences were aligned with FASTA (PEARSON 1990). Three-dimensional modeling was performed with the InsightII software (Molecular Simulations, San Diego) following a previously described procedure (KRÜGER *et al.* 1998). The model of the *Pax6* homeodomain was docked to its DNA

recognition site, guided by the atomic coordinates of the paired/DNA complex (WILSON *et al.* 1995).

Expression of Pax6 homeodomains of the wild-type and Pax6^{4Neu} alleles in bacteria: The appropriate fragments were amplified from cDNA templates and inserted between the *Pst*I and *Hind*III sites of the pQE-41 vector (QIAGEN). The expression constructs result in the in-frame fusion of the desired sequence (the Pax6 amino acids 218 to 288, which includes the homeodomain and six amino acid residues upstream and four amino acid residues downstream) to the C-terminal end of the mouse dihydrofolate reductase protein. The pQE expression constructs were transformed into *Escherichia coli* strain M15 (pREP4), which carries the *lacI^q* repressor gene. Cultures of exponentially growing bacteria were induced with 0.1 mM isopropyl thiogalactoside for 2 hr at 30°. Bacterial pellets were lysed in 50 mM NaH₂PO₄, 300 mM NaCl, pH 8.0, 0.5 mg/ml lysozyme, 5 µg/ml DNaseI and 1 mM phenylmethylsulfonyl fluoride. Crude extracts were electrophoresed in 10% SDS-PAGE and proteins were visualized by staining with Coomassie brilliant blue.

Western blotting: Crude extracts were fractionated on a 10% SDS-PAGE and then electrophoretically transferred to fluorotrans membranes (Pall Europe Ltd, Portsmouth, UK) and probed with rabbit anti-Pax6-homeodomain antiserum (1:200; serum 13, gift from Dr. S. Saule, Institut Pasteur de Lille), which was detected with anti-rabbit IgG alkaline phosphatase conjugate (1:1000; Promega, Madison, WI).

Electrophoretic mobility shift analysis: Crude extracts from the transformed bacteria were incubated with 15 fmol of the target oligonucleotide, which was 3' end-labeled with digoxigenin-11-ddUTP as recommended by the supplier (Roche Diagnostics, Mannheim, Germany). The target oligonucleotide contained the Pax6 homeodomain binding sequence P3 (CZERNY and BUSSLINGER 1995), in which the two halves of the palindromic sequence were separated by TGA as in the rhodopsin promoter (SHENG *et al.* 1997). The sequence of the double-strand oligonucleotide (with P3 underlined) is as follows: 5'-TCGAGGGCATCAGGATGCTAATTGAATTAGCATCCGATCGGG-3' and 3'-CCCCTAGTCCTACGATTAAGCTAATCGTAGGCTAGCCAGCT-5'.

Protein-DNA complexes were separated on a native 10% polyacrylamide gel (in 0.25× Tris-borate-EDTA), blotted onto BM nylon membranes, and detected by autoradiography following an enzyme immunoassay with antidigoxigenin (Fab)-alkaline phosphatase and the chemiluminescent substrate CSPD (Roche).

The sequence data presented in this article have been submitted to the EMBL/GenBank Data Libraries under the accession numbers: Pax6^{2Neu}, Y19193; Pax6^{3Neu}, Y19195; Pax6^{4Neu}, Y19196; Pax6^{5Neu}, Y19197; Pax6^{6Neu}, Y19198; Pax6^{7Neu}, Y19199; Pax6^{9Neu}, AJ292077; and Pax6^{10Neu}, AJ307468.

RESULTS

Mutations: Table 1 gives the original mutant identification, the proposed allele symbol (based on the molecular characterization results below), the mutagenic treatment of the parental male mice, and reference to the mutagenesis experiments in which the original mutants were recovered. Seven mutations (ENU-5011, ENU-5045, ENU-636, ENU-2033, ENU-642, TX-12, and ENU-6037) were recovered in offspring derived from fertilizations in which the participating parental male germ cells were mutagenically treated at the stem cell spermatogonial stage (fertilizations occurred >49 days after treat-

ment). The original mutant recovered for each of these independent mutations expressed bilateral anterior polar cataract, corneal adhesions, and, depending on the mutant allele, slight to more severe microphthalmia. Genetic confirmation tests indicated that the original mutants were heterozygous for an autosomal dominant allele. Two mutations (ENU-65 and nPMS-9) were recovered in offspring derived from fertilizations in which the participating parental male germ cells were mutagenically exposed at the spermatocyte stage. The fertilization producing the mutant ENU-65 occurred 24 days after treatment. The fertilization producing the mutant nPMS-9 occurred 20 days after treatment. The original mutant ENU-65 expressed unilaterally anterior polar opacity, corneal adhesions, and microphthalmia. Genetic confirmation and subsequent breeding results suggested that the original mutant was a gonosomal mosaic for an autosomal dominant mutation (FAVOR 1983; FAVOR *et al.* 1990; FAVOR and NEUHÄUSER-KLAUS 1994). The original mutant nPMS-9 expressed bilateral eye defects and genetic confirmation crosses were consistent with the assumption that the mutant was heterozygous for an autosomal dominant mutation.

The expressivity of all mutations was variable with mutant carriers expressing a range of phenotypes from small anterior polar cataracts to the more extreme phenotype of anterior polar opacity, corneal adhesions, iris abnormalities, and microphthalmia. Furthermore, the degree of phenotype expressed between the eyes of an individual mutation carrier was variable.

Examination of the eyes of animals not treated with atropin revealed that heterozygous carriers for all mutant alleles expressed greatly reduced or absent iris.

Breeding results are given in Table 2. Segregation analyses for the outcross of heterozygous carriers to wild type indicated a 1:1 ratio of wild type to mutant carrier offspring consistent with an autosomal dominant mutation without viability or penetrance effects for six mutations (Pax6^{2Neu}, Pax6^{3Neu}, Pax6^{4Neu}, Pax6^{5Neu}, Pax6^{6Neu}, and Pax6^{10Neu}). The segregation analyses of three mutations (Pax6^{7Neu}, Pax6^{8Neu}, and Pax6^{9Neu}) deviated significantly from the expected 1:1 ratio. For Pax6^{8Neu} and Pax6^{9Neu} there was an excess of wild-type offspring relative to mutants. The deviations in segregation observed for these two mutations may be due to a conservative classification of offspring in the initial generations of breeding or to genetic background effects since, as will be seen below, (a) Pax6^{8Neu} (with an observed deviation in segregation) is an exact repeat mutation of that carried by Pax6^{6Neu} (with no deviation in segregation) and (b) once the spectrum of phenotypes associated with the mutations became known we were able to classify the genotypes on the basis of phenotype with no deviation in the segregation ratio in the mapping studies. The segregation results for Pax6^{7Neu} showed an excess of mutant offspring. However, there was no deviation in the

TABLE 1

Origin and proposed allele symbols of the mouse *Pax6* mutations characterized in this study

Mutant ID	Allele symbol	Treatment ^a	Reference
ENU-5011	<i>Pax6</i> ^{2Neu}	4 × 40 mg/kg ENU	FAVOR and NEUHÄUSER-KLAUS (2000)
ENU-65	<i>Pax6</i> ^{3Neu}	250 mg/kg ENU	FAVOR (1983)
ENU-5045	<i>Pax6</i> ^{4Neu}	4 × 40 mg/kg ENU	FAVOR and NEUHÄUSER-KLAUS (2000)
ENU-636	<i>Pax6</i> ^{5Neu}	160 mg/kg ENU	FAVOR (1986)
ENU-2033	<i>Pax6</i> ^{6Neu}	2 × 80 mg/kg ENU	FAVOR and NEUHÄUSER-KLAUS (2000)
ENU-642	<i>Pax6</i> ^{7Neu}	160 mg/kg ENU	FAVOR (1986)
TX-12	<i>Pax6</i> ^{8Neu}	2 mg/kg TEM + 6 Gy	FAVOR and NEUHÄUSER-KLAUS (2000)
nPMS-9	<i>Pax6</i> ^{9Neu}	600 mg/kg nPMS	FAVOR and NEUHÄUSER-KLAUS (2000)
ENU-6037	<i>Pax6</i> ^{10Neu}	3 × 100 mg/kg ENU	Unpublished

^a ENU, ethylnitrosourea; TEM, triethylenemelamine; nPMS, *n*-propyl methanesulfonate.

segregation ratio in the mapping analyses and we conclude the deviation to be spurious.

Examination of embryos from *inter se* crosses of heterozygous carriers of seven mutations (*Pax6*^{2Neu}, *Pax6*^{3Neu}, *Pax6*^{5Neu}, *Pax6*^{6Neu}, *Pax6*^{8Neu}, *Pax6*^{9Neu}, and *Pax6*^{10Neu}) revealed that the resultant phenotypes were identical to those previously described (HOGAN *et al.* 1988): Heterozygotes express obvious microphthalmia with a triangular-shaped pupil and homozygotes express anophthalmia with severe craniofacial defects (Figure 2A). Embryos from two mutations deviated from this general phenotypic classification. *Pax6*^{4Neu} and *Pax6*^{7Neu} heterozygotes expressed abnormal pupil shape but eye size reduction was only slight; homozygous mutants were anophthalmic but some were observed to have a distinct optic pit with underlying pigmentation (Figure 2, B and C).

Mapping: Two mutations (*Pax6*^{2Neu} and *Pax6*^{3Neu}) were

shown to be alleles of *Pax6* on the basis of noncomplementation with *Pax6*^{Sey-Neu}. Phenotypic analyses of the mutation *Pax6*^{10Neu} suggested that *Pax6* was mutated. The remaining six mutations were localized relative to the chromosome 2 markers *D2Mit249* and *Agouti* (Table 3). All mutations mapped to the same region, expressed a similar phenotype, and, therefore, were assumed to be mutant alleles of the same gene. Combined mapping results yielded the following gene order: *D2Mit249*-(1.4 cM)-*Pax6*-(25.3 cM)-*Agouti*.

Molecular characterization: Sequence analyses indicated that the *Pax6* gene was affected in all nine mutations (Table 4). Seven mutations (*Pax6*^{2Neu}, *Pax6*^{4Neu}, *Pax6*^{5Neu}, *Pax6*^{6Neu}, *Pax6*^{7Neu}, *Pax6*^{8Neu}, and *Pax6*^{10Neu}) were base pair substitutions, one mutation (*Pax6*^{3Neu}) was a base pair insertion, and one mutation (*Pax6*^{9Neu}) was a 7-bp deletion.

TABLE 2

Breeding results for heterozygote *Pax6* mutant outcrosses or *inter se* crosses

Mutation	Offspring resulting from the cross				
	M/+ × +/+		M/+ × M/+		
	+/+	M/+	+/+	M/+	M/M
<i>Pax6</i> ^{2Neu}	83	67	13	32	12
<i>Pax6</i> ^{3Neu}	93	93	24	30	18
<i>Pax6</i> ^{4Neu}	64	61	5	6	4 ^a
<i>Pax6</i> ^{5Neu}	67	63	5	13	7
<i>Pax6</i> ^{6Neu}	132	127	9	13	11
<i>Pax6</i> ^{7Neu}	54	91	8	9	6 ^a
<i>Pax6</i> ^{8Neu}	221	39	4	10	4
<i>Pax6</i> ^{9Neu}	77	57	3	14	4
<i>Pax6</i> ^{10Neu}	91	90	3	5	1

Offspring from outcrosses were classified at weaning by slit lamp biomicroscopy. Embryos from *inter se* crosses were classified at E15–E17.

^a Two embryos observed with pronounced optic pits and underlying pigmentation.

TABLE 3

Mapping results of six independent dominant eye mutations of the mouse in the cross (C3H-*Pax6*^{#Neu} × C57BL/6) × C57BL/6

Markers	Haplotypes ^a							
	■	□	■	□	■	□	■	□
<i>D2Mit249</i>	■	□	■	□	■	□	■	□
<i>Pax6</i>	■	□	□	■	■	□	□	■
<i>Agouti</i>	■	□	□	■	□	■	■	□
<i>Pax6</i> ^{4Neu}	37	40	0	1	22	14	0	0
<i>Pax6</i> ^{5Neu}	39	42	0	0	9	4	0	0
<i>Pax6</i> ^{6Neu}	39	40	0	0	11	16	0	0
<i>Pax6</i> ^{7Neu}	41	30	1	1	14	15	1	2
<i>Pax6</i> ^{8Neu}	42	44	0	0	16	9	0	0
<i>Pax6</i> ^{9Neu}	43	30	0	0	14	9	1	2
Total	241	226	1	2	86	67	2	4

For each independent mutation, the number of offspring carrying the haplotypes inherited from the C3H-*Pax6*^{#Neu} × C57BL/6 outcross parent are given.

^a The solid boxes designate the alleles carried by the congenic C3H-*Pax6*^{#Neu} strains; the open boxes designate the alleles carried by inbred strain C57BL/6.

TABLE 4
Molecular characterization of *Pax6* mutations of the mouse

Allele	Mutation	Position	Codon	Domain
<i>Pax6</i> ^{2Neu}	T to C	Intron 9, 2	5' splice site After 269	Homeobox
<i>Pax6</i> ^{3Neu}	A insert	Exon 7, after 598	After 145	Linker
<i>Pax6</i> ^{4Neu}	T to C	Exon 10, 979	Ser273 to Pro	Homeobox
<i>Pax6</i> ^{5Neu}	A to T	Exon 6, 517	Arg119 to Stop	Paired box
<i>Pax6</i> ^{6Neu}	C to A	Exon 10, 1092	Tyr310 to Stop	P/S/T
<i>Pax6</i> ^{7Neu}	A to T	Exon 4, -3		Kozak sequence
<i>Pax6</i> ^{8Neu}	C to A	Exon 10, 1092	Tyr310 to Stop	P/S/T
<i>Pax6</i> ^{9Neu}	TCACAGC deletion	Exon 5, 261-267	After 33	Paired box
<i>Pax6</i> ^{10Neu}	C to T	Exon 6, 469	Gln103 to Stop	Paired box

The predicted Pax6 protein products are given in Figure 1. Seven mutations (*Pax6*^{2Neu}, *Pax6*^{3Neu}, *Pax6*^{5Neu}, *Pax6*^{6Neu}, *Pax6*^{8Neu}, *Pax6*^{9Neu}, and *Pax6*^{10Neu}) result in a truncated Pax6 protein product. *Pax6*^{2Neu} is a base pair substitution at nucleotide position 2 of the intron 9 donor splice site. The isolated cDNA was 87 bp longer than wild type due to the destruction of the splice site and the use of a cryptic splice site. Translation of the aberrant mRNA is predicted to result in a normal amino acid sequence up to codon 269 of exon 9 followed by 23 amino acids encoded by the included intron 9 sequence and a premature stop. The mutation results in the truncation of the last 15 amino acids of the C terminus of the homeodomain and the entire P/S/T domain. The *Pax6*^{3Neu} frameshift mutation results in a

normal amino acid sequence through codon 145 of exon 7 followed by 12 aberrant amino acids and a premature stop. The gene product contains a normal paired domain but the linker region, the homeodomain, and the P/S/T domain are all deleted. The base pair substitution in the *Pax6*^{5Neu} mutation creates a premature stop site in the C terminus of the paired box, resulting in a predicted gene product that is truncated for the last 27 amino acids of the paired domain as well as the linker region, the homeodomain, and the P/S/T domain. *Pax6*^{6Neu} is also a base pair substitution, which creates a premature stop codon and results in a truncated gene product from the N-terminal end of the P/S/T domain. *Pax6*^{8Neu} is a repeat mutation such as that observed in *Pax6*^{6Neu}. The 7-bp deletion associated with *Pax6*^{9Neu} is predicted to result in an extremely truncated gene product consisting of the first 32 amino acids followed by 17 aberrant amino acids and a premature stop. Finally, the *Pax6*^{10Neu} base pair substitution creates a stop codon in the C terminus of the paired box. The predicted mutant gene product consists of the first 102 amino acids and a truncation of the last 43 amino acids of the paired domain, as well as the linker region, the homeodomain, and the P/S/T region.

One missense mutation has been identified. The *Pax6*^{4Neu} mutation results in an amino acid substitution, Ser273 to Pro, in the third helix of the homeodomain. The predicted gene product contains a single amino acid substitution at a site known to be critical for DNA binding activity. Finally, the *Pax6*^{7Neu} mutation is a base pair substitution in the Kozak sequence in the 5'-untranslated region of exon 4 and is predicted to affect translation.

We detected two differences between our wild-type *Pax6* sequence and the published mouse *Pax6* sequence (WALTHER and GRUSS 1991) at position 354 (T instead of C) and at position 1263 (G instead of A). The differences do not affect the amino acids specified. Our sequence data are for strain C3H, were based upon analyses of cDNA, and were confirmed by analysis of genomic DNA. All mutant sequences have been submitted to the EMBL DNA sequence database with the following

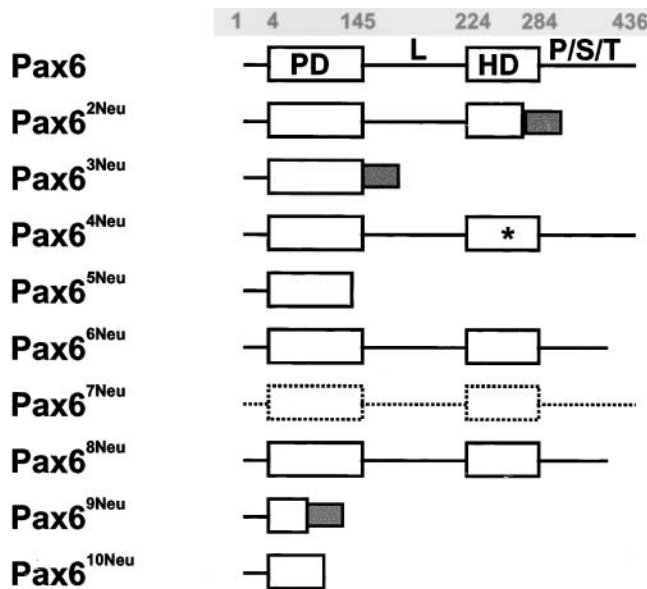


FIGURE 1.—Predicted protein product of wild-type and mutant *Pax6* alleles. PD, paired domain; L, linker region; HD, homeodomain; P/S/T, proline-/serine-/threonine-rich region (the codon positions at the domain borders of the *Pax6* wild type are shaded numbers); shaded boxes, aberrant amino acid sequences; *, missense mutation; dashed lines, reduced translation of *Pax6*^{7Neu} messenger RNA.

TABLE 5

Degree of lens/corneal opacity in *Pax6* mutation heterozygotes and wild-type litter mates

Genotype	Phenotypic class				
	0%	25%	50%	75%	100%
<i>Pax6</i> ^{3Neu} +/-		2	4	9	17
<i>Pax6</i> ^{3Neu} +/+	48				
<i>Pax6</i> ^{4Neu} +/-	6	11	5	2	
<i>Pax6</i> ^{4Neu} +/+	32				
<i>Pax6</i> ^{7Neu} +/-	9	25	6	2	
<i>Pax6</i> ^{7Neu} +/+	48				

accession numbers: *Pax6*^{2Neu}, Y19193; *Pax6*^{3Neu}, Y19195; *Pax6*^{4Neu}, Y19196; *Pax6*^{5Neu}, Y19197; *Pax6*^{6Neu}, Y19198; *Pax6*^{7Neu}, Y19199; *Pax6*^{9Neu}, AJ292077; and *Pax6*^{10Neu}, AJ307468.

Heterozygote and homozygote phenotypes of the hypomorph *Pax6*^{4Neu} and *Pax6*^{7Neu} mutant alleles: The degree of lens/corneal opacity in mutant heterozygotes and wild-type littermates is given in Table 5. Heterozygous carriers of the *Pax6*^{3Neu} truncation mutation express a severe lens/corneal opacity, the median and modal values being 100% opaque. In contrast, carriers of the two presumed hypomorph alleles *Pax6*^{4Neu} and *Pax6*^{7Neu} express a less severe phenotype. For both mutations the median and modal values were 25% opaque. As a measure of eye size, individual eyes were weighed. Data were first analyzed for the effects of mutant allele (*Pax6*^{3Neu}, *Pax6*^{4Neu}, or *Pax6*^{7Neu}), genotype (heterozygous or wild type), and sex of animal. The effects of both mutant allele ($F_{2, 196} = 6.00$, $P < 0.002$) and genotype ($F_{1, 196} = 591.07$, $P < 0.0001$) were highly significant. The sex of the animal had no effect on eye weight ($F_{1, 196} = 0.12$, $P \sim 0.729$). Data were pooled for sex of animal and the range, mean, and standard error of the mean eye weights for heterozygous carriers and wild-type littermates are given in Table 6. Eye weights of *Pax6*^{3Neu} carriers were 78% that of wild-type littermates. The corresponding values for the *Pax6*^{4Neu} and *Pax6*^{7Neu} alleles were less severe (83 and 86%, respectively). Examination of embryos from *inter se* crosses of *Pax6*^{4Neu} heterozygotes (Figure 2B) revealed that the resultant phenotypes were less severe than that observed for carriers of a *Pax6* null allele (HOGAN *et al.* 1988). We further characterized the extent of nasal development, since *Pax6* is essential for normal development of this organ (HOGAN *et al.* 1988; GRINDLEY *et al.* 1995; QUINN *et al.* 1996). Previous studies have shown that *Pax9* expression marks the mesenchymal domains of the medial and lateral nasal processes after E10.5 of mouse development (PETERS *et al.* 1998). Using the *Pax9*^{lacZ} allele as a reporter, we found that the lateral and medial nasal processes were completely absent in homozygotes for a *Pax6* null allele, while the lateral and medial nasal

TABLE 6

Eye weight (mg) in *Pax6* mutation heterozygotes and wild-type litter mates

Genotype	N	Minimum	Maximum	Mean	SEM
<i>Pax6</i> ^{3Neu} +/+	48	17	21	19.27	0.1322
<i>Pax6</i> ^{4Neu} +/-	17	13	17	15.88	0.2828
<i>Pax6</i> ^{4Neu} +/+	19	16	20	19.05	0.2474
<i>Pax6</i> ^{7Neu} +/-	42	16	18	16.71	0.0980
<i>Pax6</i> ^{7Neu} +/+	47	17	21	19.36	0.1340

processes were present but of reduced size in homozygotes for the *Pax6*^{4Neu} allele (Figure 2C). Histological examination indicated that, in comparison to homozygous wild type (Figure 3A), there was hyperplasia of the cartilaginous parts of the nasal anlage and a concomitant reduction in size of the nasal cavities and their associated nasal epithelia in homozygous *Pax6*^{4Neu} mutant embryos (Figure 3B).

The extent of eye development in homozygous mutant *Pax6*^{4Neu} and *Pax6*^{7Neu} embryos is most interesting. Whereas in homozygous wild type (Figure 3A) eye development is complete, with a well-developed retina and lens, eye development in homozygous mutants terminated prematurely (Figure 3, B–E). The optic stalk is not in contact with the surface ectoderm. However, the tip of the optic stalk is enlarged and invaginated to form a “pseudo-optic cup.” In homozygous mutant *Pax6*^{4Neu} embryos, the enlarged and invaginated tip of the optic stalk is surrounded by cartilage. Invaginations from the surface ectoderm are evident but remain a considerable distance from the tip of the optic stalk. Lens did not develop. Homozygotes for *Pax6* null mutations die shortly after birth. In contrast, homozygous *Pax6*^{4Neu} and *Pax6*^{7Neu} offspring survive up to 24–36 hr after birth. Together, the above observations suggest *Pax6*^{4Neu} and *Pax6*^{7Neu} are hypomorph alleles.

Three-dimensional model and DNA-binding activity of the *Pax6*^{4Neu} mutant gene product: The site of the *Pax6*^{4Neu} missense mutation, Ser273, is located in the third helix of the homeodomain (position 50 in the homeodomain, position 9 in the third helix). The substitution of Pro for Ser is predicted to interrupt the structure of the third helix (Figure 4), which, in three-dimensional structures of homologous homeodomain proteins complexed with DNA, inserts into the major groove of the DNA target. We compared the binding activity of the wild type and *Pax6*^{4Neu} mutant homeodomains to the palindromic P3 target oligonucleotide, since the *Pax6* homeodomain binds specifically to the P3 sequence (CZERNY and BUSSLINGER 1995). Comparable concentrations of wild-type and mutant homeodomain proteins were assayed (Figure 5A). The binding activity of the *Pax6*^{4Neu} homeodomain to the P3 oligonucleotide was shown to

be greatly reduced in comparison to the binding activity of the wild-type homeodomain (Figure 5B). Only very faint traces of monomer protein-DNA complex were observed. The mutant protein competes weakly with the wild-type protein, reducing the level of dimer protein-DNA complex formation.

Levels of Pax6 expression in homozygous *Pax6*^{4Neu} and *Pax6*^{7Neu} mutant mice: The levels of Pax6 expression in homozygous mutant embryos are given in Figure 6. In comparison to homozygous wild-type embryos, normal levels of Pax6 expression were observed in homozygous *Pax6*^{4Neu} embryos. For homozygous *Pax6*^{7Neu} mutant embryos, the level of Pax6 expression was greatly reduced. The lack of signal associated with homozygous *Pax6*^{3Neu} embryos can be taken only as a negative control for the Western blot since the *Pax6*^{3Neu} truncation mutation

results in loss of the homeodomain against which the anti-Pax6 antiserum reacts.

DISCUSSION

Here we have extended the *Pax6* allelic series in the mouse. We have shown by mapping, molecular characterization, and phenotype analyses that seven alleles result in truncated gene products and express phenotypic defects characteristic for null mutations. Most importantly, we have identified two potential hypomorph alleles.

Truncation mutations: Six *Pax6* mutations have been previously described. The *Pax6*^{LacZ} (ST-ONGE *et al.* 1997) was constructed and the initiation start site as well as the entire paired box were replaced by the β-galactosidase reporter gene and the neo-selector gene. *Pax6*^{Sey-Dey} is due to an intergenic deletion including the *Pax6* and *Wt1* genes (GLASER *et al.* 1990). *Pax6*^{Sey} is a base pair substitution creating a premature stop codon in the linker region (HILL *et al.* 1991). *Pax6*^{Sey-Neu} is a splice site mutation resulting in a predicted gene product truncated from the N-terminal end of the P/S/T region (HILL *et al.* 1991). *Pax6*^{Coop} is a base pair substitution that creates a premature stop codon between the homeodomain and the P/S/T region (LYON *et al.* 2000). *Pax6*^{Sey-H} is a large deletion and most likely involves additional linked loci (HILL *et al.* 1991). Together with the presently described mutations, an allelic series exists for truncation mutations with the order from the longest gene product to total gene ablation as follows: *Pax6*^{Sey-Neu}, *Pax6*^{6Neu}, *Pax6*^{Coop}, *Pax6*^{2Neu}, *Pax6*^{Sey}, *Pax6*^{3Neu}, *Pax6*^{5Neu}, *Pax6*^{10Neu}, *Pax6*^{9Neu}, and *Pax6*^{LacZ}. LYON *et al.* (2000) have observed very small vestiges of unpigmented eyes in homozygous *Pax6*^{Coop} embryos, raising the possibility that this mutation may be a hypomorph allele. Although a direct comparison of the phenotypic effects of the different *Pax6* alleles in one laboratory has not been

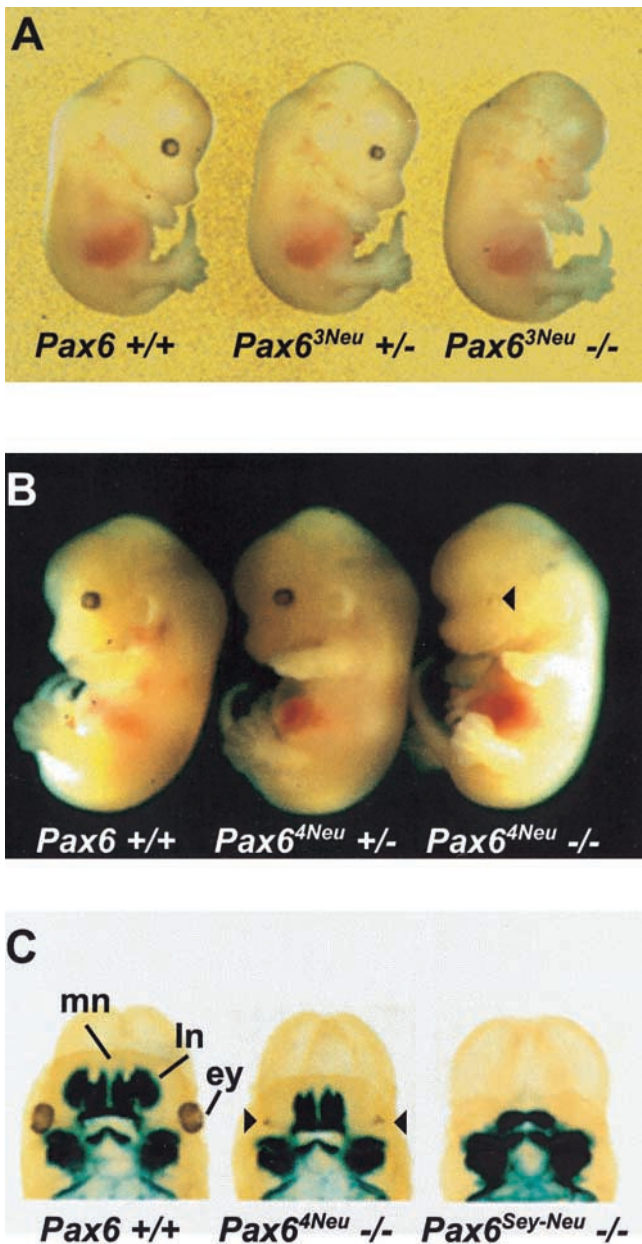
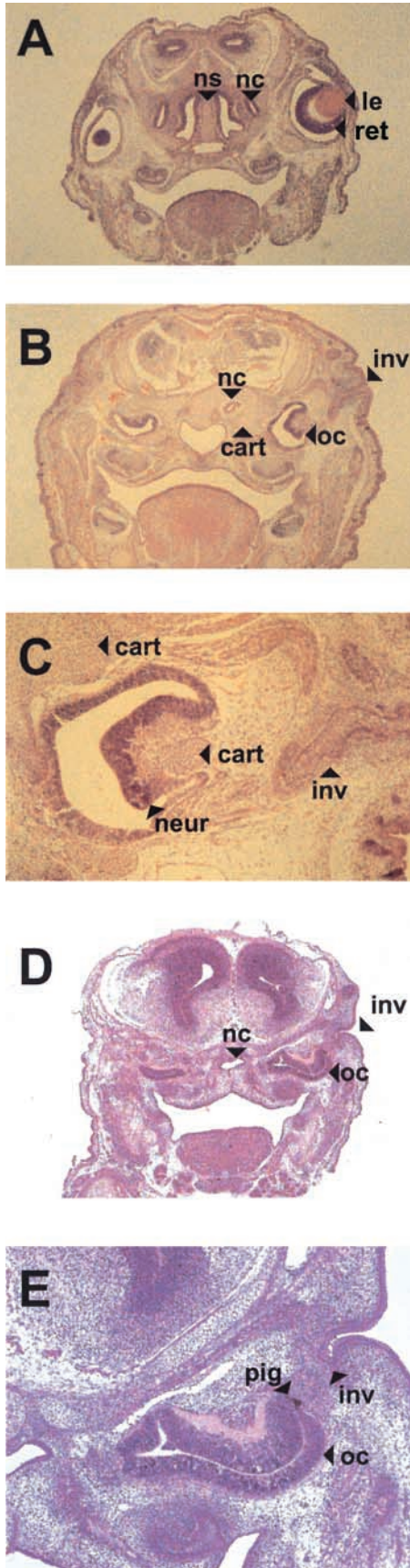


FIGURE 2.—Phenotypic characterization of wild-type, heterozygous, and homozygous mutant *Pax6* embryos. (A) Homozygous wild-type, heterozygous, and homozygous mutant *Pax6*^{3Neu} embryos (E15) expressing the typical phenotypes for a *Pax6* null allele. Heterozygotes have a clearly smaller eye with a distinctive triangular shaped pupil. Homozygous mutants are anophthalmic. (B) *Pax6*^{4Neu} embryos (E15) expressing the phenotypes for a *Pax6* hypomorph allele. Heterozygotes are distinguishable from wild types only by the slight distortion in the shape of the eye. Homozygous mutants develop a rudimentary, pigmented eye (arrow). (C) Assay for nasal development in homozygous *Pax6* mutant embryos (E12) employing the expression of the *Pax9*^{LacZ} reporter gene in nasal mesenchyme of *Pax9*^{LacZ} ^{+/+} embryos. As compared to homozygous wild type, homozygotes for the hypomorph *Pax6*^{4Neu} allele have reduced lateral (ln) and medial (mn) nasal processes. The rudimentary, pigmented eye in the *Pax6*^{4Neu} homozygote (arrows) can also be seen. The lateral and medial nasal processes are completely absent in homozygotes for the *Pax6*^{Sey-Neu} null allele (right). ey, eye.



carried out, some appropriate data are available. In homozygous *Pax6*^{Sev} and *Pax6*^{Sev-Neu} mutants, the optic stalk develops distally, there is a condensation of mesenchymal-like cells underneath the surface ectoderm, and the overlying surface ectoderm appears to form a pit, but neither a lens nor an eye develops (GRINDLEY *et al.* 1995; SCHEDL *et al.* 1996). We observed pits in the presumptive eye region of homozygous embryos for all mutations reported here, including the shortest truncation allele in which none of the Pax6 domains remain intact. Thus, the development of such pits may be a component of the phenotype associated with null alleles. The gross morphology of heterozygous and homozygous carriers of all truncation alleles reported here is similar, which suggests that *Pax6* gene function requires all domains to be intact. Destruction of the paired domain or the homeodomain should lead to loss of gene function since each participates directly in DNA binding. The amino acid composition of the P/S/T region of the Pax6 protein resembles the activation domains of the transcription factors Oct-1 and Oct-2 (TANAKA and HERR 1990). Such activation domains are important for the interaction of DNA-bound transcription factors with other proteins required for transcription.

Potential hypomorph alleles: In homozygous *Pax6* null mutants the optic vesicle makes initial contact with the surface ectoderm but their contact is subsequently

FIGURE 3.—The extent of eye and nasal development in wild-type and homozygous E16 *Pax6*^{4Neu} or *Pax6*^{7Neu} mutant embryos. (A) Homozygous wild type showing a well-developed eye with lens (le) and retina (ret) and normal nasal structure with nasal septum (ns) and nasal cavities (nc). (B) Homozygous *Pax6*^{4Neu} mutant showing premature termination of eye development and abnormal nasal development. The tip of the optic stalk is a considerable distance from the surface ectoderm. At the tip of the optic stalk an enlargement and invagination of the neuroectoderm form a pseudo-optic cup (oc). From the surface ectoderm there is an invagination (inv) that does not make contact with the pseudo-optic cup and a lens does not develop. The pseudo-optic cup is surrounded by cartilage (cart), which is an extension of the hyperplastic nasal cartilage. Development of the nasal organ is characterized by a hyperplasia of the cartilage, no nasal septum, and only rudimentary nasal cavities (nc). (C) Enlargement of the pseudo-optic cup region in the homozygous *Pax6*^{4Neu} mutant embryo from B, showing the invaginated neuroectoderm of the tip of the optic stalk (neur), lack of contact between the tip of the optic stalk and the invaginated surface ectoderm (inv), and the cartilaginous structures (cart) surrounding the tip of the enlarged and invaginated optic stalk. (D) Homozygous *Pax6*^{7Neu} mutant embryo. Premature eye development and abnormal nasal development are similar to that observed for the *Pax6*^{4Neu} mutation, although hyperplasia of the nasal cartilage was not observed. (E) Enlargement of the pseudo-optic cup region in the homozygous *Pax6*^{7Neu} mutant embryo from D. The invaginated neuroectoderm of the tip of the optic stalk and a lack of contact between the tip of the optic stalk and the invaginated surface ectoderm were similar to that seen in homozygous *Pax6*^{4Neu} mutant embryos. Pigmented cells (pig) can be seen in the region of the pseudo-optic cup.

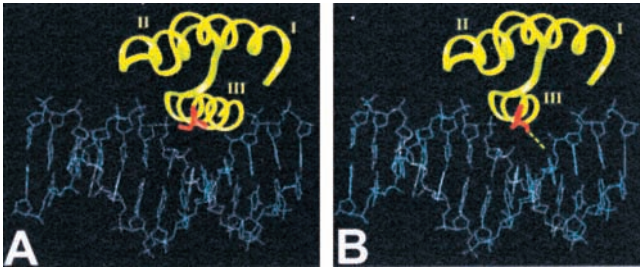


FIGURE 4.—Three-dimensional model of the *Pax6* homeodomain (green) docked to the DNA recognition sequence (cyan). The protein is represented as a backbone ribbon. The position of the mutated residue 9 is marked in red. (A) Wild-type homeodomain with the recognition α -helix inserted into the DNA major groove. (B) In the mutant *Pax6*^{4Neu} homeodomain the substitution of serine to proline leads to disruption of the recognition α -helix such that the DNA major groove cannot be recognized.

lost. The tip of the optic vesicle is broader but does not invaginate in the early steps of optic cup formation and the surface ectoderm does not thicken or invaginate, a process that normally marks the early steps of lens formation (HOGAN *et al.* 1986; SCHMAHL *et al.* 1993; GRINDLEY *et al.* 1995). Studies utilizing chimeric mice have demonstrated that Pax6 activity is essential for surface ectoderm cells to participate in lens formation (QUINN *et al.* 1996). Our preliminary description of homozygous *Pax6*^{4Neu} and *Pax6*^{7Neu} mutants indicates that eye development proceeds further than that observed for homozygous null mutations. Both the tip of the optic vesicle and the surface ectoderm invaginate. However, contact is not maintained and neither a lens nor a true optic cup develops.

The most conserved segment of the 300 homeodomains known to date is helix III, which makes extensive DNA contacts in the major groove of the DNA target sequence (GEHRING *et al.* 1994). In all *Pax6* homologs, residue 9 of the third helix is serine. Mutagenesis studies *in vitro* have confirmed that the amino acid at position 9 of the third helix is a major determinant for the DNA-binding specificity of the homeodomain (HANES and BRENT 1989; TREISMAN *et al.* 1989). The interaction of the N-terminal end of the Pax6 homeodomain and the minor groove of the P3 target sequence has been observed in structural studies (GEHRING *et al.* 1994; QIAN *et al.* 1994b). Cooperative dimerization is a two-step process that cannot take place without an efficient monomer binding event (WILSON *et al.* 1993). Thus our observation of faint traces of *Pax6*^{4Neu} mutant monomer protein-DNA complex may be due to the weak interaction of the intact N-terminal end of the homeodomain with the minor groove of the target DNA.

The *Pax6*^{7Neu} allele is an A-to-T transversion in the 5'-untranslated mRNA region, at position -3 of the Kozak sequence that surrounds the translation start codon. From a survey of 699 vertebrate mRNAs for the initiation

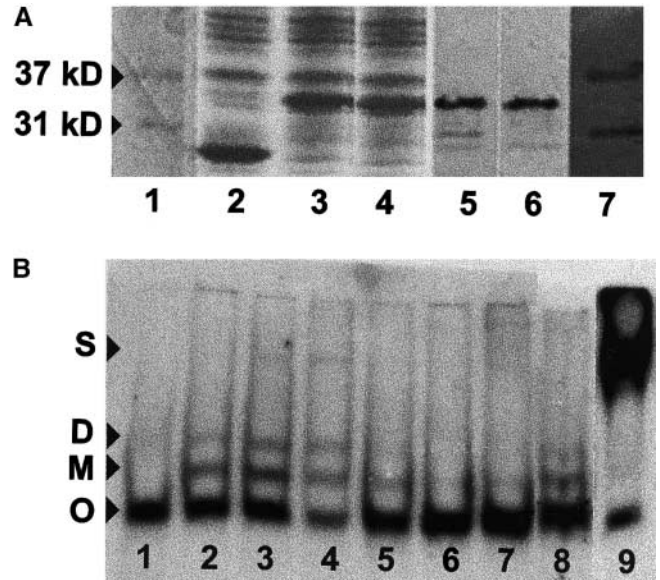


FIGURE 5.—DNA-binding assay of the wild-type and mutant Pax6 homeodomain. (A) SDS-PAGE and Western blot analysis of the homeodomain of *Pax6* wild-type and mutant *Pax6*^{4Neu} alleles expressed in *E. coli* as fusion proteins. The efficiency of expression was similar for wild-type and mutant alleles as observed by SDS-PAGE (lanes 1–4) and Western blotting (lanes 5–7). To determine the amounts of protein, Coomassie staining intensities of 3 μ l of 1:10 and 1:50 crude lysate were compared with known amounts of marker proteins. For the Western blots a *Pax6*-homeodomain-specific antiserum was used (gift from Dr. S. Saule, Institut Pasteur de Lille). Lane 1, marker; lane 2, vector; lane 3, wild type; lane 4, *Pax6*^{4Neu}; lane 5, wild type; lane 6, *Pax6*^{4Neu}; lane 7, marker. (B) DNA-binding properties of the homeodomain of *Pax6* wild-type and mutant *Pax6*^{4Neu} alleles analyzed by electrophoretic mobility shift assay. The target oligonucleotide was P3. Whole cell extracts from the transformed *E. coli* strain M15pREP4 were incubated with 15 fmol of the digoxigenin-labeled P3 oligonucleotide. Binding specificity was demonstrated by competition of the labeled oligonucleotide with an excess of unlabeled oligonucleotide and by a supershift assay with Pax6 homeodomain-specific antibody. Lane 1, oligonucleotide alone; lanes 2–4, oligonucleotide with the wild-type *Pax6* homeodomain (25, 50, or 100 ng, respectively); lane 5, as lane 4 with 1.5 pmol unlabeled oligonucleotide; lanes 6–7, oligonucleotide with the mutant *Pax6*^{4Neu} homeodomain (50 or 100 ng, respectively); lane 8, oligonucleotide with 100 ng wild type and 100 ng *Pax6*^{4Neu} homeodomain; lane 9, as lane 4 with 2 μ l of the *Pax6*-homeodomain-specific antiserum. The positions of the free oligonucleotide (O), the monomeric (M) and dimeric (D) DNA-protein complexes, and the antibody DNA-protein complex shifted band (S) are marked.

site, CC(A/G)CCaugG emerged as the consensus sequence (KOZAK 1987a). Within this consensus motif the purine at position -3 is the most highly conserved in all eukaryotic mRNAs and mutations at this position affect translation more profoundly than point mutations at other positions (KOZAK 1986). In the absence of a purine at position -3, however, a G residue following the AUG codon (position +4) is essential for efficient translation (KOZAK 1987b).

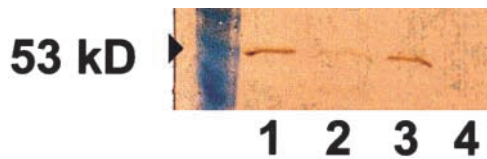


FIGURE 6.—Levels of Pax6 expression in wild-type and homozygous mutant embryos. Protein extracts from heads of E15 embryos were analyzed by Western blot for Pax6 expression. Estimation of protein concentration, electrophoresis procedures, and Pax6-homeodomain-specific antiserum were as given in Figure 5. Fourteen micrograms of total protein were electrophoresed per lane. Lane 1, *Pax6* +/+; lane 2, *Pax6*^{7Neu} -/-; lane 3, *Pax6*^{4Neu} -/-; lane 4, *Pax6*^{3Neu} -/-.

The sequence surrounding the AUG translation start site, CCAGCaugC, (WALTHER and GRUSS 1991) in the wild-type *Pax6* gene agrees well with the Kozak consensus sequence. The transversion of A to T at position -3 of the Kozak sequence in *Pax6*^{7Neu} combined with C at position +4 suggests that the efficiency of translation is reduced. The reduced levels of Pax6 product in the Western blot analysis confirmed this prediction. Our observation of homozygous mutant embryos with rudimentary eyes suggests that the mutation *Pax6*^{7Neu} retains some Pax6 rest activity and may represent a hypomorph allele.

Human PAX6 mutation database: Human patients expressing aniridia, Peters' anomaly, congenital cataract, keratitis, or foveal hypoplasia have been shown to be heterozygous carriers of PAX6 mutations (GLASER *et al.* 1992, 1994; JORDAN *et al.* 1992; EPSTEIN *et al.* 1994; HANSON *et al.* 1994; MIRZAYANS *et al.* 1995; AZUMA *et al.* 1996). In addition, one patient expressing anophthalmia and CNS defects has been shown to be a compound heterozygote for PAX6 mutations (GLASER *et al.* 1994). A database of human PAX6 mutations has been created (BROWN *et al.* 1998) and recently reviewed (<http://www.hgu.mrc.ac.uk/Softdata/PAX6>). A total of 201 mutations were considered, of which 143 were base pair substitutions, 56 were small deletions, insertions, or deletion/insertions, one was a large deletion, and one was a CA repeat in an intron. The majority of mutations were predicted to result in premature termination of translation and 38 missense mutations were recovered. Most of the recovered missense mutations expressed total aniridia similar to truncation alleles. However, some missense mutations expressed an intermediate phenotype. The mutation R26G (Arg to Gly) was described as a hypomorph allele (TANG *et al.* 1997) and the mutation A33P (Ala to Pro) was associated with a partial aniridia with significant iris remnants (HANSON *et al.* 1999). Both mutations are in the N terminus of the paired domain, which is involved in the binding to the paired domain target DNA. The missense mutations A79E (Ala to Glu) in the paired domain and R208Q (Arg to Gln) in the linker region express a milder phenotype

(GRØNSKOV *et al.* 1999). Only one missense mutation in the homeobox was detected, Q255H (Gln to His), at a highly conserved site in the recognition helix. The mutation is likely a hypomorph allele since it is associated with sporadic aniridia (CHAO *et al.* 2000). The value of an extensive allelic series of mouse *Pax6* mutations is that it provides animal models with which to study in detail gene function in development. The hypomorph mutant alleles may be of special interest for studying the effect of a Pax6 gene product dose on the resulting phenotypes that develop. Our continued efforts to characterize dominant eye mutations recovered in mutagenesis experiments in the mouse should lead to the identification of additional *Pax6* mutant alleles.

We thank Bianca Hildebrand and Irmgard Zaus for their expert technical assistance; Utz Linzner, Institute of Pathology/BIODV Workgroup, for the synthesis of the oligonucleotide primers; and Professor S. Saule for the gift of the rabbit anti-mouse-Pax6-homeodomain. The Tskgel DNA-NPR-S ion exchange column for the HPLC purification of PCR products was kindly provided by TosoHaas, Stuttgart, Germany. Research was supported in part by contract no. CHR-X-CT93-0181 from the Commission of the European Communities and National Institutes of Health grant R01EY10321.

LITERATURE CITED

- AZUMA, N., S. NISHINA, H. YANAGISAWA, T. OKUYAMA and M. YAMADA, 1996 PAX6 missense mutation in isolated foveal hypoplasia. *Nat. Genet.* **13**: 141-142.
- BENTLEY, C. A., M. P. ZIDEHSARAL, J. C. GRINDLEY, A. F. PARLOW, S. BARTH-HALL *et al.*, 1999 Pax6 is implicated in murine pituitary endocrine function. *Endocrine* **10**: 171-177.
- BROWN, A., M. MCKIE, V. VAN HEYNINGEN and J. PROSSER, 1998 The human PAX6 mutation database. *Nucleic Acids Res.* **26**: 259-264.
- CHAO, L. Y., V. HUFF, L. C. STRONG and G. F. SAUNDERS, 2000 Mutation in the PAX6 gene in twenty patients with aniridia. *Hum. Mutat.* **15**: 332-339.
- CZERNY, T., and M. BUSSLINGER, 1995 DNA-binding and transactivation properties of Pax-6: three amino acids in the paired domain are responsible for the different sequence recognition of Pax-6 and BSAP (Pax-5). *Mol. Cell. Biol.* **15**: 2858-2871.
- EPSTEIN, J. A., T. GLASER, J. CAI, L. JEPEAL, D. S. WALTON *et al.*, 1994 Two independent and interactive DNA-binding subdomains of the Pax6 paired domain are regulated by alternative splicing. *Genes Dev.* **8**: 2022-2034.
- FAVOR, J., 1983 A comparison of the dominant cataract and recessive specific-locus mutation rates induced by treatment of male mice with ethylnitrosourea. *Mutat. Res.* **110**: 367-382.
- FAVOR, J., 1986 The frequency of dominant cataract and recessive specific-locus mutations in mice derived from 80 and 160 mg ethylnitrosourea per kg body weight treated spermatogonia. *Mutat. Res.* **162**: 69-80.
- FAVOR, J., and A. NEUHÄUSER-KLAUS, 1994 Genetic mosaicism in the house mouse. *Annu. Rev. Genet.* **28**: 27-47.
- FAVOR, J., and A. NEUHÄUSER-KLAUS, 2000 Saturation mutagenesis for dominant eye morphological defects in the mouse *Mus musculus*. *Mamm. Genome* **11**: 520-525.
- FAVOR, J., A. NEUHÄUSER-KLAUS and U. H. EHLING, 1990 The frequency of dominant cataract and recessive specific-locus mutations and mutation mosaics in F₁ mice derived from post-spermatogonial treatment with ethylnitrosourea. *Mutat. Res.* **229**: 105-114.
- FAVOR, J., P. GRIMES, A. NEUHÄUSER-KLAUS, W. PRETSCH and D. STAMBOLIAN, 1997 The mouse *Cat4* locus maps to Chromosome 8 and mutants express lens-corneal adhesion. *Mamm. Genome* **8**: 403-406.
- GEHRING, W. J., Y. Q. QIAN, M. BILLETER, K. FURUKUBO-TOKUNAGA,

- A. F. SCHIER *et al.*, 1994 Homeodomain-DNA recognition. *Cell* **78**: 211–223.
- GLASER, T., J. LANE and D. HOUSMAN, 1990 A mouse model of the aniridia-Wilms tumor deletion syndrome. *Science* **250**: 823–827.
- GLASER, T., D. S. WALTON and R. L. MAAS, 1992 Genomic structure, evolutionary conservation and aniridia mutations in the human *PAX6* gene. *Nat. Genet.* **2**: 232–239.
- GLASER, T., L. JEPEAL, J. G. EDWARDS, S. R. YOUNG, J. FAVOR *et al.*, 1994 *PAX6* gene dosage effect in a family with congenital cataracts, aniridia, anophthalmia and central nervous system defects. *Nat. Genet.* **7**: 463–471.
- GOSSLER, A., and J. ZACHGO, 1993 Gene and enhancer trap screens in ES cell chimeras, pp. 181–227 in *Gene Targeting: A Practical Approach*, edited by A. L. JOYNER. Oxford University Press, New York.
- GÖTZ, M., A. STOYKOVA and P. GRUSS, 1998 *Pax6* controls radial glia differentiation in the cerebral cortex. *Neuron* **21**: 1031–1044.
- GRINDLEY, J. C., D. R. DAVIDSON and R. E. HILL, 1995 The role of *Pax-6* in eye and nasal development. *Development* **121**: 1433–1442.
- GRINDLEY, J. C., L. K. HARGETT, R. E. HILL, A. ROSS and B. L. HOGAN, 1997 Disruption of *Pax6* function in mice homozygous for the *Pax6^{Sey-1Nex}* mutation produces abnormalities in the early development and regionalization of the diencephalon. *Mech. Dev.* **64**: 111–126.
- GRØNSKOV, K., T. ROSENBERG, A. SAND and K. BRØNDUM-NIELSEN, 1999 Mutational analysis of *PAX6*: 16 novel mutations including 5 missense mutations with a mild aniridia phenotype. *Eur. J. Hum. Genet.* **7**: 274–286.
- HANES, S. D., and R. BRENT, 1989 DNA specificity of the Bicoid activator protein is determined by homeodomain recognition helix residue 9. *Cell* **57**: 1275–1283.
- HANSON, I. M., J. M. FLETCHER, T. JORDAN, A. BROWN, D. TAYLOR *et al.*, 1994 Mutations at the *PAX6* locus are found in heterogeneous anterior segment malformations including Peters' anomaly. *Nat. Genet.* **6**: 168–173.
- HANSON, I., A. CHURCHILL, J. LOVE, R. AXTON, T. MOORE *et al.*, 1999 Missense mutations in the most ancient residues of the *PAX6* paired domain underlie a spectrum of human congenital eye malformations. *Hum. Mol. Genet.* **8**: 165–172.
- HEINZMANN, U., J. FAVOR, J. PLENDL and G. GREVERS, 1991 Entwicklungsstörung des olfaktorischen Organs. Ein Beitrag zur kausalen Genese bei einer Mausmutante. *Verh. Anat. Ges.* **85** (Anat. Anz. Suppl. 170): 511–512.
- HILL, R. E., J. FAVOR, B. L. M. HOGAN, C. C. T. TON, G. F. SAUNDERS *et al.*, 1991 Mouse *Small eye* results from mutations in a paired-like homeobox-containing gene. *Nature* **354**: 522–525.
- HOGAN, B. L. M., G. HORSBURGH, J. COHEN, C. M. HETHERINGTON, G. FISHER *et al.*, 1986 *Small eyes (Sey)*: a homozygous lethal mutation on chromosome 2 which affects the differentiation of both lens and nasal placodes in the mouse. *J. Embryol. Exp. Morphol.* **97**: 95–110.
- HOGAN, B. L. M., E. M. A. HIRST, G. HORSBURGH and C. M. HETHERINGTON, 1988 *Small eye (Sey)*: a mouse model for the genetic analysis of craniofacial abnormalities. *Development* **103**(Suppl.): 115–119.
- HRABÉ DE ANGELIS, M., H. FLASWINKEL, H. FUCHS, B. RATHKOLB, D. SOEWARTO *et al.*, 2000 Genome-wide, large-scale production of mutant mice by ENU mutagenesis. *Nat. Genet.* **25**: 444–447.
- JORDAN, T., I. HANSON, D. ZALETAYEV, S. HODGSON, J. PROSSER *et al.*, 1992 The human *PAX6* gene is mutated in two patients with aniridia. *Nat. Genet.* **1**: 328–332.
- KAUFMAN, M. H., H.-H. CHANG and J. P. SHAW, 1995 Craniofacial abnormalities in homozygous *Small eye (Sey/Sey)* embryos and newborn mice. *J. Anat.* **186**: 607–617.
- KIOUSSI, C., S. O'CONNELL, L. ST-ONGE, M. TREIER, A. S. GLEIBERMAN *et al.*, 1999 *Pax6* is essential for establishing ventral-dorsal cell boundaries in pituitary gland development. *Proc. Natl. Acad. Sci. USA* **96**: 14378–14382.
- KISSINGER, C. R., B. LIU, E. MARTIN-BLANCO, T. B. KORNBERG and C. O. PABO, 1990 Crystal structure of an engrailed homeodomain-DNA complex at 2.8 Å resolution: a framework for understanding homeodomain-DNA interactions. *Cell* **63**: 579–590.
- KOZAK, M., 1986 Point mutations define a sequence flanking the AUG initiator codon that modulates translation by eukaryotic ribosomes. *Cell* **44**: 283–292.
- KOZAK, M., 1987a An analysis of 5'-noncoding sequences from 699 vertebrate messenger RNAs. *Nucleic Acids Res.* **15**: 8125–8148.
- KOZAK, M., 1987b At least six nucleotides preceding the AUG initiator codon enhance translation in mammalian cells. *J. Mol. Biol.* **196**: 947–950.
- KRÜGER, K., T. HERMANN, V. ARMBRUSTER and F. PFEIFER, 1998 The transcriptional activator GvpE for the halobacterial gas vesicle genes resembles a basic region leucine-zipper regulatory protein. *J. Mol. Biol.* **279**: 761–771.
- LYON, M. F., D. BOGANI, Y. BOYD, P. GUILLOT and J. FAVOR, 2000 Further genetic analysis of two autosomal dominant mouse eye defects, *Ccw* and *Pax6^{cop}*. *Mol. Vis.* **6**: 199–203.
- MANLY, K. F., 1993 A Macintosh program for storage and analysis of experimental genetic mapping data. *Mamm. Genome* **4**: 303–313.
- MIRZAYANS, F., W. G. PEARCE, I. M. MACDONALD and M. A. WALTER, 1995 Mutation of the *PAX6* gene in patients with autosomal dominant keratitis. *Am. J. Hum. Genet.* **57**: 539–548.
- NOLAN, P. M., J. PETERS, M. STRIVENS, D. ROGERS, J. HAGAN *et al.*, 2000 A systematic, genome-wide, phenotype-driven mutagenesis programme for gene function studies in the mouse. *Nat. Genet.* **25**: 440–443.
- PEARSON, W. R., 1990 Rapid and sensitive sequence comparison with FASTP and FASTA, pp. 63–98 in *Methods in Enzymology*, Vol. 183, edited by R. F. DOOLITTLE. Academic Press, San Diego.
- PETERS, H., A. NEUBÜSER, K. KRATOCHWIL and R. BALLING, 1998 *Pax6* deficient mice lack pharyngeal pouch derivatives and teeth and exhibit craniofacial and limb abnormalities. *Genes Dev.* **12**: 2735–2747.
- PROSSER, J., and V. VAN HEYNINGEN, 1998 *PAX6* mutations reviewed. *Hum. Mutat.* **11**: 93–108.
- QIAN, Y. Q., K. FURUKUBO-TOKUNAGA, D. RESENDEZ-PEREZ, M. MÜLLER, W. J. GEHRING *et al.*, 1994a Nuclear magnetic resonance solution structure of the fushi tarazu homeodomain from *Drosophila* and comparison with the Antennapedia homeodomain. *J. Mol. Biol.* **238**: 333–345.
- QIAN, Y. Q., D. RESENDEZ-PEREZ, W. J. GEHRING and K. WÜTHRICH, 1994b The des(1–6)Antennapedia homeodomain: comparison of the NMR solution structure and the DNA-binding affinity with the intact Antennapedia homeodomain. *Proc. Natl. Acad. Sci. USA* **91**: 4091–4095.
- QUINN, J. C., J. D. WEST and R. E. HILL, 1996 Multiple functions for *Pax6* in mouse eye and nasal development. *Genes Dev.* **10**: 435–446.
- SCHEDL, A., A. ROSS, M. LEE, D. ENGELKAMP, P. RASHBASS *et al.*, 1996 Influence of *PAX6* gene dosage on development: overexpression causes severe eye abnormalities. *Cell* **86**: 71–82.
- SCHMAHL, W., M. KNOEDLSER, J. FAVOR and D. DAVIDSON, 1993 Defects of neuronal migration and the pathogenesis of cortical malformations are associated with *Small eye (Sey)* in the mouse, a point mutation at the *Pax-6*-locus. *Acta Neuropathol.* **86**: 126–135.
- SHENG, G., E. THOUVENOT, D. SCHMUCKER, D. S. WILSON and C. DESPLAN, 1997 Direct regulation of *rhodopsin 1* by *Pax-6*/eyeless in *Drosophila*: evidence for a conserved function in photoreceptors. *Genes Dev.* **11**: 1122–1131.
- ST-ONGE, L., B. SOSA-PINEDA, K. CHOWDHURY, A. MANSOURI and P. GRUSS, 1997 *Pax6* is required for the differentiation of glucagon-producing α -cells in mouse pancreas. *Nature* **387**: 406–409.
- STOYKOVA, A., R. FRITSCH, C. WALTHER and P. GRUSS, 1996 Forebrain patterning defects in *Small eye* mutant mice. *Development* **122**: 3453–3465.
- STOYKOVA, A., M. GÖTZ, P. GRUSS and J. PRICE, 1997 *Pax6*-dependent regulation of adhesive patterning, *R-cadherin* expression and boundary formation in developing forebrain. *Development* **124**: 3765–3777.
- STOYKOVA, A., D. TREICHEL, M. HALLONET and P. GRUSS, 2000 *Pax6* modulates the dorsoventral patterning of the mammalian telencephalon. *J. Neurosci.* **20**: 8042–8050.
- TANAKA, M., and W. HERR, 1990 Differential transcriptional activation by Oct-1 and Oct-2: interdependent activation domains induce Oct-2 phosphorylation. *Cell* **60**: 375–386.
- TANG, H. K., L. Y. CHAO and G. F. SAUNDERS, 1997 Functional analysis of paired box missense mutations in the *PAX6* gene. *Hum. Mol. Genet.* **6**: 381–386.
- THEILER, K., D. S. VARNUM and L. C. STEVENS, 1978 Development of Dickie's small eye, a mutation in the house mouse. *Anat. Embryol.* **155**: 81–86.

- TREISMAN, J., P. GÖNCZY, M. VASHISHTHA, E. HARRIS and C. DESPLAN, 1989 A single amino acid can determine the DNA binding specificity of homeodomain proteins. *Cell* **59**: 553–562.
- TSAO, D. H., J. M. GRUSCHUS, L. H. WANG, M. NIRENBERG and J. A. FERRETTI, 1995 The three-dimensional solution structure of the NK-2 homeodomain from *Drosophila*. *J. Mol. Biol.* **251**: 297–307.
- WALTHER, C., and P. GRUSS, 1991 *Pax-6*, a murine paired box gene, is expressed in the developing CNS. *Development* **113**: 1435–1449.
- WILSON, D., G. SHENG, T. LECUIT, N. DOSTATNI and C. DESPLAN, 1993 Cooperative dimerization of paired class homeo domains on DNA. *Genes Dev.* **7**: 2120–2134.
- WILSON, D. S., B. GUENTHER, C. DESPLAN and J. KURIYAN, 1995 High resolution crystal structure of a paired (Pax) class cooperative homeodomain dimer on DNA. *Cell* **82**: 709–719.

Communicating editor: C. KOZAK